

Spectroscopic and structural studies on adducts of silver(I) cyanide with ER₃ ligands (E = P, As or Sb)

Graham A. Bowmaker,^a Effendy,^{b,c} Jason C. Reid,^a Clifton E. F. Rickard,^a Brian W. Skelton^b and Allan H. White^b

^a Department of Chemistry, University of Auckland, Private Bag 92019, Auckland, New Zealand

^b Department of Chemistry, The University of Western Australia, Nedlands, W.A. 6907, Australia

^c Jurusan Pendidikan Kimia, FPMIPA IKIP, Malang, Jalan Surabaya 6, Malang, 65145, Indonesia

The adducts AgCN:EPh₃ (E = P, As or Sb) (1:2) and AgCN:PPh₃ (1:1) have been characterized by room temperature single crystal structure determination and low frequency vibrational spectroscopy. The compounds AgCN:EPh₃ (E = P or As) (1:2) [as pyridine (py) monosolvates] are isomorphous and of the form [(Ph₃E)₃-Ag(CN)Ag(EPh₃)₃][Ag(CN)₂], an aqua-2-methylpyridine solvate and an acetonitrile solvate also being structurally characterized for the E = P adduct. For E = Sb the complex is a simple single stranded polymer ... Ag(SbPh₃)₂(CN)Ag(SbPh₃)₂(CN) ... as is AgCN:PPh₃ (1:1), ... Ag(PPh₃)₂(CN)Ag(CN)Ag(PPh₃)₂ An adduct of the form AgCN:PR₃ (1:1) is also obtained for tris(2,4,6-trimethoxyphenyl)phosphine (tmpp) as a pyridine hemisolvate, now ionic but with the pyridine loosely co-ordinated to the anion, [Ag(tmpp)₂][Ag(CN)₂(py)]. By contrast, in the AgCN:P(*o*-tol)₃ (tol = *o*-tolyl):py(1:0.5:0.5) adduct, Ag{P(*o*-tol)₃}⁺(py) moieties are linked in a single-stranded polymer by NCAgCN units, ... Ag[P(*o*-tol)₃](py)(NCAgCN) The structural characterization of [Ag(PPh₃)₃(CN)] has also been made. The far-infrared spectra of AgCN·2AgNO₃, [Ag(SbPh₃)₂(CN)] and [Ag(SbPh₃)₃(CN)] show ν(AgX) bands (X = CN) at 435, 358 and 310 cm⁻¹. The relationship between the ν(AgX) wavenumbers and the Ag–X bond lengths *r*(AgX) for the case of terminally bound CN groups has been established, and this has the same form as that found previously for a range of AgX complexes (X = Cl, Br or I) with phosphine and arsine ligands. The ν(AgX) wavenumbers for the CN-bridged compounds AgCN·2AgNO₃ and [Ag(SbPh₃)₂(CN)] are about 50 cm⁻¹ higher than those for compounds with terminal Ag–CN bonds of similar bond length. Similar behaviour is observed for the bridging CN groups in the cations of the ionic 1:2 complexes [{Ag(EPh₃)₃}₂CN]⁺[Ag(CN)₂]⁻·3py (E = P or As), where the ν(AgX) wavenumbers (301, 354 cm⁻¹ respectively) are about 80 cm⁻¹ higher than those predicted for terminal bonding.

Structurally defined adducts of silver(I) cyanide with Group V unidentate donors are very sparse, being restricted to a recent report of the 1:3 triphenylstibine adduct [Ag(SbPh₃)₃(CN)],¹ presumably a consequence of a tendency of such species to polymerize by virtue of the ambidentate nature of the cyanide ligand. In recent work^{2,3} we have extended the array to 1:1 and 1:2 adducts with tricyclohexylarsine, the 1:1 adduct obtained in various forms being one-stranded infinitely polymeric. We have extended these studies to encompass further ligand types, and record here syntheses, room temperature single crystal determinations, and low frequency vibrational spectroscopy for adducts of silver cyanide with bases of the form EPh₃ for E = P, As or Sb of 1:2 AgCN:EPh₃ stoichiometry, and of 1:1 stoichiometry for E = P, defining novel species incorporating bridging cyanide moieties, most being solvated by non-co-ordinating pyridine base. Adducts of 1:1 and 1:0.5 stoichiometry, whose characterization rests on X-ray studies, have also been obtained with tmpp [= tris(2,4,6-trimethoxyphenyl)phosphine] and P(*o*-tol)₃ (*o*-tol = *o*-tolyl) solvated with pyridine, but with the pyridine more or less co-ordinated, yielding novel arrays in these instances. We record the results of these studies herein, together with the structure determination of [Ag(PPh₃)₃(CN)].

Experimental

Syntheses

Colourless crystalline materials were obtained in all cases by dissolving appropriate millimolar stoichiometries of silver(I) cyanide and pnictogen ER₃ base in pyridine base (5–10 cm³) with warming and allowing to cool slowly, in some cases

crystalline material depositing only after volume reduction by evaporation. The materials are generally solvated, the solvent in most cases being readily lost, so that useful analyses were obtained for a limited number of species only, AgCN:PPh₃:py (1:2:1) (Found: C, 67.6; H, 5.0; N, 4.0. C₄₂H₃₅AgN₂P₂ requires C, 68.40; H, 4.78; N, 3.80%) and AgCN:AsPh₃:py (1:2:1) (Found: C, 60.6; H, 4.5; N, 3.6. C₄₂H₃₅AgAs₂N₂ requires C, 61.11; H, 4.27; N, 3.39%). Crystals for the X-ray work were mounted in capillaries. In addition to the general method involving reactions carried out in pyridine base as described above, the following products, obtained from acetonitrile solvent, require explicit comment.

[(Ph₃P)₃Ag(CN)Ag(PPh₃)₃][Ag(CN)₂]-2MeCN and [(Ph₃P)₂-Ag(CN)Ag(CN)]_n. Silver cyanide (0.265 g, 2.0 mmol) and PPh₃ (1.558 g, 6.0 mmol) were dissolved, with stirring, in boiling MeCN (10 cm³). The resultant solution was filtered, and on cooling a mixture of white 'needle-like' crystals and white 'cube-shaped' crystals formed in the filtrate. A portion of the product was filtered off and air-dried. During the drying process the cube-shaped crystals rapidly became opaque. Some of the needle-like white crystals were physically separated from the bulk of the dried sample and subjected to an X-ray study, showing them to be a 1:1 AgCN:PPh₃ complex. A 'cube-shaped' specimen was collected from the mother-liquor for an X-ray study, and determined to be the 1:2 AgCN:PPh₃ adduct, [{Ag(PPh₃)₃}₂CN][Ag(CN)₂]-2MeCN.

[Ag(SbPh₃)₂CN]. This was prepared by dissolution of AgCN (0.094 g, 0.70 mmol) and SbPh₃ (0.773 g, 2.2 mmol) in boiling MeCN (25 cm³). The resultant solution was filtered, and on

cooling white crystals of the complex formed in the filtrate. M.p. 147–151 °C (Found: C, 53.0; H, 3.4; N, 1.6. C₃₇H₃₀AgNSb₂ requires C, 52.90; H, 3.60; N, 1.67%). This sample was shown by X-ray diffraction measurements to be identical to that obtained from pyridine solution.

AgCN·2AgNO₃. This complex was prepared for IR studies by the following reaction: AgNO₃ (3.42 g, 20 mmol) was dissolved in water (10 cm³). To the resulting solution was added AgCN (1.34 g, 10 mmol). The mixture was stirred, with heating for 4 h. After this time some of the AgCN remained undissolved, and the solution was filtered. Upon cooling, fine white crystals of the complex formed in the filtrate. These were filtered off. Yield 0.335 g (Found: C, 2.6; H, 0.0; N, 8.6. CAg₃N₃O₆ requires C, 2.54; H, 0.00; N, 8.87%).

Structure determinations

General procedures and caveats concerning cyanide modelling are given in ref. 3, specific details as follows; as a general particular caveat here we reiterate a common inability to distinguish cyanide C, N atoms crystallographically in bridging arrays, which were modelled as composites.

(a) AgCN:EPh₃:py (1:2:1) (×3) ≡ [(Ph₃E)₃Ag(CN)Ag(EPh₃)₃][Ag(CN)₂]₃·3solv. ≡ C₁₁₁H₉₀Ag₃E₆N₃·3solv. (*i*) solv = py, *E* = P or As. Triclinic, space group P $\bar{1}$ (*C*₁¹, no. 2), *Z* = 1.

α (E = P). C₁₂₆H₁₀₅Ag₃P₆N₆, *M* = 2212.8, *a* = 15.335(6), *b* = 14.338(5), *c* = 13.45(1) Å, α = 69.30(5), β = 85.56(6), γ = 85.69(3)°, *U* = 2755 Å³, *D_c* = 1.33 g cm⁻³, *F*(000) = 1134, μ_{Mo} = 6.0 cm⁻¹, specimen 0.26 × 0.40 × 0.65 mm, *A*_{min,max}^{*} = 1.16, 1.24, 2 θ_{max} = 50°, *N* = 9653, *N_o* = 5809, *R* = 0.046, *R'* = 0.048.

β (E = As). C₁₂₆H₁₀₅Ag₃As₆N₆, *M* = 2476.5, *a* = 15.482(4), *b* = 14.414(3), *c* = 13.650(6) Å, α = 68.80(3), β = 86.06(3), γ = 85.83(2)°, *U* = 2830 Å³, *D_c* = 1.45 g cm⁻³, *F*(000) = 1242, μ_{Mo} = 22.0 cm⁻¹, specimen 0.22 × 0.22 × 0.41 mm, *A*_{min,max}^{*} = 1.50, 1.63, 2 θ_{max} = 45°, *N* = 7280, *N_o* = 3699, *R* = 0.050, *R'* = 0.050.

Variata. One of the pyridine solvent molecules is disposed about a crystallographic inversion centre, modelled with C/N composites at the putative nitrogen sites (both E = P/As).

(*ii*) 3S = 2(2-Methylpyridine) = C₇H₇N·H₂O. C₁₂₃H₁₀₆Ag₃P₆N₅O, *M* = 2179.7, triclinic, space group P $\bar{1}$, *a* = 25.847(6), *b* = 14.743(5), *c* = 14.545(3) Å, α = 85.48(3), β = 84.96(2), γ = 79.79(3)°, *U* = 5422 Å³, *D_c* (*Z* = 2) = 1.34 g cm⁻³, *F*(000) = 2236, μ_{Mo} = 6.8 cm⁻¹, specimen 0.55 × 0.20 × 0.26 mm, *A*_{min,max}^{*} = 1.13, 1.19, 2 θ_{max} = 47.5°, *N* = 15 688, *N_o* = 8489, *R* = 0.049, *R'* = 0.050.

Variata. Solvent molecules were modelled as shown, the 2-methylpyridine groups being modelled as constrained geometry rigid bodies, two being disordered about crystallographic inversion centres, and site occupancies set at unity after trial refinement. The bridging cyanide was modelled as disordered about a crystallographic inversion centre.

(b) AgCN:PPh₃:MeCN (1:2:2/3) (×3) ≡ [Ag(PPh₃)₃]₂·CN][Ag(CN)₂]₂·2Me₃CN. C₁₁₅H₉₆Ag₃N₅P₆, *M* = 2057.4, triclinic, space group P $\bar{1}$, *a* = 13.635(3), *b* = 13.934(3), *c* = 16.747(3) Å, α = 98.92(3), β = 110.04(3), γ = 112.95(3)°, *U* = 2595 Å³, *D_c* (*Z* = 2) = 1.317 g cm⁻³, *F*(000) = 1052, μ_{Mo} = 7.0 cm⁻¹, specimen 0.55 × 0.46 × 0.38 mm, 2 θ_{max} = 58°, *N* = 11 515, *N_o* = 10 417, *R* = 0.037, *R'* = 0.130.

Variata. Data were collected on a Siemens SMART diffractometer with a CCD area detector at a sample temperature of 203(2) K. A full sphere of data was collected by a series of ω scans and a semiempirical absorption correction applied by comparing equivalent reflections. The bridging cyanide ion lies on a centre of symmetry and was refined using composite scattering forms. The silver atom of the [Ag(CN)₂]⁻ group

also lies on a centre of symmetry and the cyanide group was modelled as C-bound.

(c) AgCN:SbPh₃ (1:2). C₃₇H₃₀AgNSb₂, *M* = 840.0, monoclinic, space group *P*2₁/*c* (*C*_{2h}⁵, no. 14), *a* = 14.249(5), *b* = 9.314(5), *c* = 28.81(1) Å, β = 117.55(2)°, *U* = 3390 Å³, *D_c* (*Z* = 4) = 1.65 g cm⁻³, *F*(000) = 1428, μ_{Mo} = 20.1 cm⁻¹, specimen 0.29 × 0.96 × 0.40 mm, *A*_{min,max}^{*} = 1.52, 2.51, 2 θ_{max} = 50°, *N* = 5943, *N_o* = 4495, *R* = 0.048, *R'* = 0.057.

Variata. Phenyl ring 22 was modelled as disordered over two sets of sites, occupancies set at 0.5 each after trial refinement, isotropic thermal parameter forms being used for the disordered atoms. Refinement behaviour suggests localization of C, N of the cyanide bridge in this case as shown, consistent with different bond lengths to the silver.

(d) AgCN:PPh₃ (1:1) (×2). C₃₈H₃₀Ag₂N₂P₂, *M* = 792.4, monoclinic, space group *P*2₁/*c*, *a* = 9.708(2), *b* = 20.159(8), *c* = 19.152(4) Å, β = 114.96(2)°, *U* = 3398 Å³, *D_c* (*Z* = 4) = 1.55 g cm⁻³, *F*(000) = 1584, μ_{Mo} = 12.8 cm⁻¹, specimen 0.28 × 0.32 × 0.09, *A*_{min,max}^{*} = 1.14, 1.22, 2 θ_{max} = 60°, *N* = 7988, *N_o* = 4437, *R* = 0.046, *R'* = 0.047.

Variata. Cyanide C, N were indistinguishable on the basis of refinement, but were modelled as C-bound within the NCAgCN component.

(e) AgCN:P(o-tol)₃:py (1:0.5:0.5) (×2). C₂₈H₂₆Ag₂N₃P, *M* = 651.2, monoclinic, space group *P*2₁/*c*, *a* = 10.335(8), *b* = 19.823(4), *c* = 15.340(4) Å, β = 90.16(4)°, *U* = 3143 Å³, *D_c* (*Z* = 4) = 1.54 g cm⁻³, *F*(000) = 1296, μ_{Mo} = 13.2 cm⁻¹, specimen 0.42 × 0.16 × 0.28 mm, *A*_{min,max}^{*} = 1.21, 1.42, 2 θ_{max} = 50°, *N* = 5520, *N_o* = 3518, *R* = 0.036, *R'* = 0.036.

Variata. Atoms C, N were assigned as localized, consistent with an NCAgCN component model, on the basis of refinement behaviour.

(f) AgCN:tmpp:py (1:1:0.5) (×2) = [Ag(tmpp)₂][Ag(CN)₂(py)]. C₆₁H₇₁Ag₂N₃O₁₈P₂, *M* = 1412, monoclinic, space group *C*2/*c* (*C*_{2h}⁶, no. 15), *a* = 19.229(6), *b* = 22.672(3), *c* = 16.08(1) Å, β = 115.47(4)°, *U* = 6327 Å³, *D_c* = 1.48 g cm⁻³, *F*(000) = 2904, μ_{Mo} = 7.4 cm⁻¹, specimen 0.25 × 0.08 × 0.41, *A*_{min,max}^{*} = 1.06, 1.24, 2 θ_{max} = 50°, *N* = 4943, *N_o* = 2974, *R* = 0.047, *R'* = 0.044.

Variata. In space group *C*2/*c* the anion is modelled with the pyridine, disposed on a crystallographic 2 axis, approaching the (NC)Ag(CN) anion normal to its quasi-axis. The silver atom is slightly displaced from the 2 axis, Ag···Ag being 0.28(2) Å; although thermal motion of associated atoms is large, no associated disorder was resolvable. Cyanide C, N were assigned as localized on the basis of refinement behaviour within the NCAgCN component.

(g) AgCN:PPh₃ (1:3). C₅₅H₄₅AgNP₃, *M* = 920.8, monoclinic, space group *P*2₁/*n* (*C*_{2h}⁵, no. 14, variant), *a* = 18.843(7), *b* = 13.748(6), *c* = 17.630(3) Å, β = 95.69(2)°, *U* = 4545 Å³, *D_c* (*Z* = 4) = 1.35 g cm⁻³, *F*(000) = 1896, μ_{Mo} = 5.2 cm⁻¹, specimen 0.10 × 0.12 × 0.40 mm, *A*_{min,max}^{*} = 1.05, 1.07, 2 θ_{max} = 50°, *N* = 7983, *N_o* = 3313, *R* = 0.048, *R'* = 0.042.

Variata. As described elsewhere¹ this complex is isomorphous with a considerable family of [Ag(EPh₃)₃X] arrays, and was refined in the setting described therein; C, N were assigned as localized on the basis of refinement behaviour, the anion being modelled as C-bound.

CCDC reference number 186/985.

See <http://www.rsc.org/suppdata/dt/1998/2139/> for crystallographic files in .cif format.

Spectroscopy

Infrared spectra were recorded at 4 cm⁻¹ resolution as Nujol

Table 1 Selected geometries (distances in Å, angles in °) for [Ag(PPh₃)₃(CN)]. Values for the isomorphous E = Sb analogue (second entry, from ref. 1) are given for comparison

Ag–C	2.148(8), 2.09(3)	Ag–P(2)	2.539(2), 2.737(2)
C–N	1.14(1), 1.14(4)	Ag–P(3)	2.529(2), 2.734(2)
Ag–P(1)	3.087(2), 2.843(3)		
N–C–Ag	175.7(8), 177(2)	P(1)–Ag–P(2)	104.89(7), 105.62(7)
C–Ag–P(1)	100.4(2), 106.8(5)	P(1)–Ag–P(3)	100.97(6), 103.38(6)
C–Ag–P(2)	117.0(2), 116.8(5)	P(2)–Ag–P(3)	115.87(9), 107.83(7)
C–Ag–P(3)	114.3(2), 115.1(6)		
Angles Ag–P(<i>n</i>)–C(<i>n</i> 11, <i>n</i> 21, <i>n</i> 31) are: <i>n</i> = 1, 109.8(2), 108.2(3), 130.0(3); <i>n</i> = 2, 112.3(2), 119.3(2), 114.2(2); <i>n</i> = 3, 114.7(2), 114.8(2), 115.4(2)°.			

mulls between KBr plates on a Digilab FTS-60 Fourier transform spectrometer employing an uncooled deuteriotriglycine sulfate detector. Far-infrared spectra were recorded at 4 cm⁻¹ resolution at room temperature as polythene discs on a Digilab FTS-60 Fourier transform infrared spectrometer employing an FTS-60V vacuum optical bench with a 6.25 μm mylar film beam splitter or a 5 lines mm⁻¹ wire mesh beam splitter, a mercury lamp source and a pyroelectric triglycine sulfate detector.

Results and discussion

Crystal structures

Adducts of silver(I) cyanide with Group V tertiary unidentate bases ER₃, E ≠ N, have been defined for a number of stoichiometries 1:*n*; in a number of cases the compounds have been obtained only with difficulty, as single crystals in isolation among a bulk matrix possibly composed of mixtures of various poly- or oligo-meric species rather than specimens representative of bulk samples. In cases where the latter have been obtained, usually from a pyridine base solution, solvation is frequent with the solvent often being lost rather readily under ambient conditions.

For *n* = 3, only the SbPh₃ adduct is recorded in the literature as a structurally characterized example;¹ in the course of the present work the PPh₃ analogue was isolated in small quantities from pyridine solution, its structure determination being recorded herewith. The structural parameters for the PPh₃ and SbPh₃ complexes are compared in Table 1. Despite the limited data available for the PPh₃ complex (only the structure), the result is of considerable interest. The complex crystallizes in a form widespread throughout [Ag(EPh₃)₃X] arrays (no copper analogues in this form are known), being monoclinic, *P*2₁/*n*, *Z* = 4, one independent molecule comprising the asymmetric unit of the structure, refinement indicating not entirely unambiguously (thermal motion on the peripheral atom being rather high) that the cyanide moiety is linearly C-(rather than N-) bound. This *P*2₁/*n* array is the most common form thus far defined for unsolvated [M(EPh₃)₃X], and is found (for M = Ag) for E = P and X = CN (here), I, NCO, ONO₂ or FBF₃, for E = As and X = Br, I, NCO, SCN or ONO₂ and for E = Sb and X = I, CN, ONO₂ or SCN, as tabulated in ref. 1 (interestingly, the example E = As, X = CN as yet is not recorded). This structural type is remarkable among those generally found for [M(EPh₃)₃X] arrays, by virtue of the substantial perturbations from 3*m* symmetry found in the E₃MX environment and confirmed at low temperature for the E = P iodide recently.⁴ While, seemingly, the general effect must be ascribed to lattice forces, it is of interest that here, in the context of what is probably the most tightly bound anionic moiety, the excursions are at their most extreme [*e.g.*, *cf.* the E = P iodide⁵ where Ag–P are 2.780(3), 2.573(2), 2.544(2) Å at room temperature] with

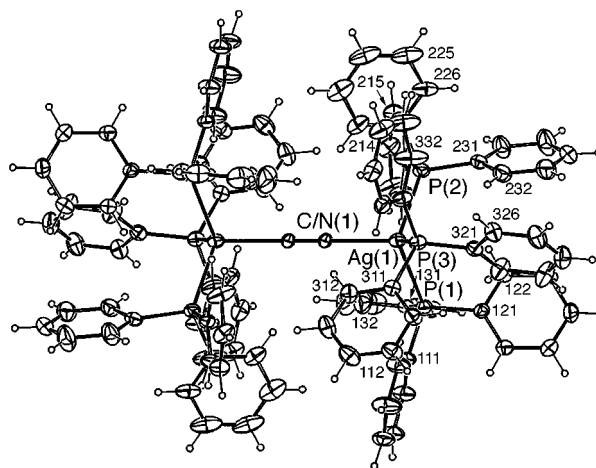


Fig. 1 Projection of the [(Ph₃P)₃Ag(CN)Ag(PPh₃)₃]⁺ cation normal to the Ag...Ag axis, as in the [Ag(CN)₂]⁻ tris(pyridine) solvate array. Cations of the arsenic and the bis(2-methylpyridine) aqua solvate analogues are similar

Ag–P(1) well on the way to dissociation; for the CAgP(1,2) array here, the angle sum is 347.2°. By contrast, in the E = Sb cyanide (see Table 1), Ag–E are more similar with angles about the phosphorus rather more tetrahedral; residual strain is still evident, inasmuch as Ag–Sb(1)–C(131) is 133.3(5)°, *cf.* 130.0(3)° in the present compound.

For *n* = 2 the present work defines the totality of the array for E = P, As or Sb. Unlike the silver halide 1:2 counterparts,^{6,7} the present are not discrete mono- or bi-nuclear entities, but, rather more complex ionic (E = P or As) or polymeric aggregates. As crystallized from pyridine, solutions of 1:2 AgCN:EPh₃ (E = P or As) yield isomorphous adducts of 1:2:1 AgCN:EPh₃:py stoichiometry, the array being ionic μ-cyano-bis{tris[triphenylphosphine(arsine)silver(i)]} dicyanoargentate tris(pyridine) solvate, [(Ph₃E)₃Ag(CN)Ag(EPh₃)₃][(NC)Ag(CN)]·3py, one half of this array modelling the asymmetric unit of the structure, entailing the location of crystallographic inversion centres at the centres of cation, anion and one of the pyridine moieties, with concomitant disorder of the nitrogen atoms of the bridging cyanides of the cations with their associated carbon atoms, and that of the centrosymmetric pyridine, with its inversion-related carbon; the central silver atom of the centrosymmetric anion is also located on a crystallographic inversion centre. The structure of the [(Ph₃P)₃Ag(CN)Ag(PPh₃)₃]⁺ cation in the E = P pyridine solvate is shown in Fig. 1. The corresponding complex crystallized from 2-methylpyridine is not isomorphous, but is nevertheless similarly formulated with three solvent molecules, modelled as two 2-methylpyridine and one adventitious water molecule; in this structure the cation and solvent molecules do not conform to any crystallographic symmetry, but there are two independent anions, one with the silver atom located at a crystallographic centre of symmetry and the other located near a crystallographic centre of symmetry as modelled in the present space group, the two components of the silver atom being separated by 1.47 Å. By contrast, the E = P adduct crystallized from acetonitrile, although not isomorphous with the pyridine solvates, shows the same centrosymmetric character as the latter, but with only two solvate (MeCN) molecules in the unit cell. Geometries about the cationic silver atoms for these species are proposed in Table 2; given the deficiency in Table 1 in respect of data for any comparable arsenic complex, the present array would seem to offer the possibility of an alternative approach to its access. However, the comparability of the phosphine complex data between Tables 1 and 2 is poor, in consequence of the previously noted perturbations; the data of Table 2, showing greater evenness in the parameters of the various metal atom environments, appear to offer a more useful approach to

Table 2 Selected geometries (distances in Å, angles in °) for $[(\text{Ph}_3\text{E})_3\text{Ag}(\text{CN})\text{Ag}(\text{EPh}_3)]^+$. Values are given in the following order: silver atoms 1, 2 of the E = P 2-methylpyridine solvate; the silver atom of the E = P acetonitrile solvate; the silver atom of the E = P, As pyridine solvates

Ag–C/N	2.27(1), 2.26(1); 2.279(3); 2.27(1), 2.19(1)
Ag–E(1)	2.572(2), 2.554(2); 2.550(2); 2.572(2), 2.612(2)
Ag–E(2)	2.560(2), 2.567(2); 2.5635(9); 2.559(2), 2.608(2)
Ag–E(3)	2.550(2), 2.564(2); 2.5869(10); 2.573(2), 2.619(2)
C/N–Ag–E(1)	107.2(3), 107.6(3); 108.47(8); 108.6(2), 110.6(3)
C/N–Ag–E(2)	105.0(3), 106.0(3); 110.72(7); 106.7(2), 109.4(3)
C/N–Ag–E(3)	105.5(4), 104.7(3); 101.80(7); 104.8(2), 105.6(3)
E(1)–Ag–E(2)	112.68(7), 112.95(7); 111.62(4); 113.24(6), 111.59(6)
E(1)–Ag–E(3)	112.83(7), 112.28(7); 112.42(4); 111.57(6), 109.84(6)
E(2)–Ag–E(3)	112.88(7), 112.60(7); 111.36(4); 111.34(5), 109.63(5)

Table 3 Selected geometries (distances in Å, angles in °) of $\text{AgCN}:\text{SbPh}_3$ (1:2). Primed atoms belong to the adjoining moiety

Ag–C	2.133(7)	Ag–Sb(2)	2.794(1)
Ag–N'	2.263(7)	C–N	1.122(9)
Ag–Sb(1)	2.7208(9)		
Ag–C–N	174.4(5)	C–Ag–Sb(2)	112.9(2)
C–N–Ag'	168.7(6)	N'–Ag–Sb(1)	104.6(2)
C–Ag–N'	115.7(5)	N'–Ag–Sb(2)	91.7(2)
C–Ag–Sb(1)	120.6(2)	Sb(1)–Ag–Sb(2)	107.24(4)

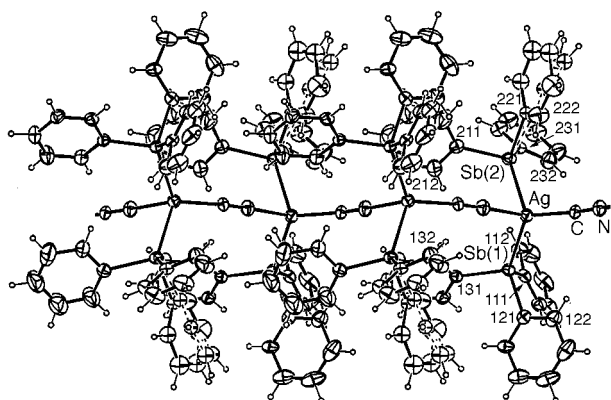


Fig. 2 Projection of the $\text{AgCN}:\text{SbPh}_3$ (1:2) polymer, normal to the polymer axis

E_3AgCN metal environment parameters, and, in this context, data for E = Sb are lacking. Of interest, despite the putative disorder in the CN bridge, is the suggestion that $\langle\text{Ag}-\text{E}\rangle$ increases on passing from E = P to E = As adducts, accompanied by a diminution in Ag–C/N. Although the cations in these complexes provide the first examples of the unusual linearly bridged silver complexes $[\{\text{Ag}(\text{EPh}_3)_2\}_2\text{CN}]^+$, it may be noted that an analogous copper(i) species, with the tetracyanoethylene radical anion as the counter ion, has recently been reported.⁸

As noted above, the 1:2 E = Sb adduct does not conform to the E = P or As ionic structural type, but, instead, is an infinite one dimensional polymer $-\text{Ag}(\text{SbPh}_3)_2-\text{CN}-\text{Ag}(\text{SbPh}_3)_2-\text{CN}-$, one $\text{Ag}(\text{SbPh}_3)_2(\text{CN})$ unit comprising the asymmetric unit, with the polymer generated by the (short) 2_1 screw axis, b , of space group $P2_1/c$ (Fig. 2). Here the refinement behaviour suggests the C, N components of the cyanide bridge to be localized as shown, with a significant disparity in Ag–C, N (Table 3), and C–Ag–Sb(x) significantly larger than N'–Ag–Sb(x). In view of the expected relative strength of the silver–cyanide interaction, the angle Sb–Ag–Sb, near the tetrahedral value, may be considered larger than expected.

For the 1:1 $\text{AgCN}:\text{ER}_3$ complexes the E = P, R = Ph array (obtained from acetonitrile solution) is the only structurally

Table 4 Selected geometries (distances in Å, angles in °) of $\text{AgCN}:\text{PPh}_3$ (1:1) [$\text{Ag}(1)$ only]

Ag(1)–N(1)	2.274(7)	Ag(1)–P(1)	2.466(2)
Ag(1)–N(2)	2.380(5)	Ag(1)–P(2)	2.471(2)
N(1)–Ag–N(2)	99.6(2)	N–Ag–P(1)	101.4(2)
N(1)–Ag–P(1)	116.8(2)	N(2)–Ag–P(2)	109.8(2)
N(1)–Ag–P(2)	103.5(1)	P(1)–Ag–P(2)	123.45(6)

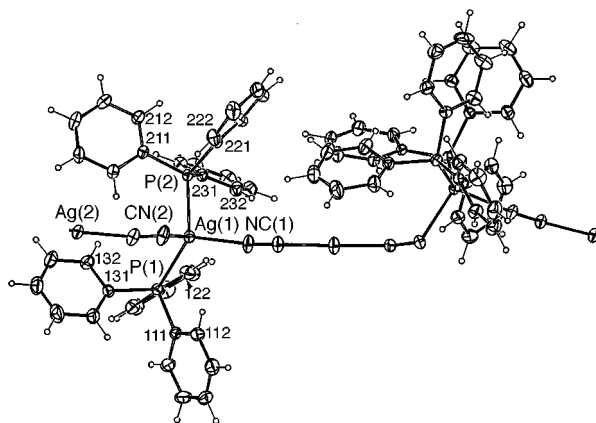


Fig. 3 Projection of the $\text{AgCN}:\text{PPh}_3$ (1:1) ($\times 2$) polymer, normal to the polymer axis

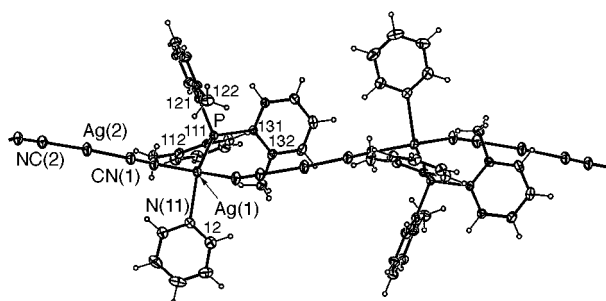


Fig. 4 Projection of the $\text{AgCN}:\text{P}(o\text{-tol})_3:\text{py}$ (2:1:1) polymer, normal to its axis

defined example. The PPh_3 complex, found in unsolvated form, is augmented by the example with tris(2,4,6-trimethoxyphenyl)-phosphine, the latter being a solvated ionic array, with the pyridine solvent molecule having an incipient co-ordinating role (see below). The $\text{AgCN}:\text{PPh}_3$ (1:1) compound is, like $\text{AgCN}:\text{SbPh}_3$ (1:2), a one dimensional polymer $-\text{Ag}(\text{PPh}_3)_2-\text{NC}-\text{Ag}-\text{CN}-$, also in space group $P2_1/c$, with the generator now the unit a translation, with $\text{Ag}(\text{EPh}_3)_2$ units spaced this time not by simple CN anionic units, but by NCAgCN anionic moieties (Fig. 3). In the latter, the assignment of C, N atoms is not clear-cut, despite the disparity of Ag(1)–C/N distances, and they are modelled as disordered. Of considerable interest here is the closing of the C/N–Ag–C/N angle about Ag(1), *vis-à-vis* the enlargement of the opposite P–Ag–P angle (Table 4).

A related structure is observed for the 1:0.5:0.5 adduct of AgCN with $\text{P}(o\text{-tol})_3$ and pyridine. Adducts of $\text{AgX}:\text{PPh}_3:\text{py}$ base (1:1:1) stoichiometry are well known and generally of binuclear $[(\text{Ph}_3\text{P})(\text{py base})\text{Ag}(\mu\text{-X})_2\text{Ag}(\text{py base})(\text{PPh}_3)]$ form with four-co-ordinate silver(i).⁹ In the present case a linear polymer of the form $-\text{Ag}(\text{PR}_3)(\text{py})-\text{NC}-\text{Ag}-\text{CN}-$ is found, also with four-co-ordinate silver(i), similar to that of the $\text{AgCN}:\text{SbPh}_3$ (1:2) adduct, but with the stoichiometry reduced to $\text{AgX}:\text{ER}_3$ (1:0.5) by subsuming the additional AgCN unit required into a bridging NCAgCN unit, modelled with C–Ag bonds on the basis of the refinement behaviour (Fig. 4). Within the anionic NCAgCN unit the geometries are largely as expected: Ag(2)–C(1,2) 2.065(6), 2.063(6), C–N (anions 1,2)

Table 5 Selected geometries (distances in Å, angles in °) of AgCN:P(*o*-tol);py (2:1:1)

Ag(1)–N(1)	2.288(5)	Ag(1)–N(11)	2.375(5)
Ag(1)–N(2')	2.332(5)	Ag(1)–P	2.451(2)
N(1)–Ag(1)–N(2')	111.1(2)	N(2')–Ag(1)–N(11)	95.1(2)
N(1)–Ag(1)–N(11)	96.3(2)	N(2')–Ag(1)–P	106.8(1)
N(1)–Ag(1)–P	118.6(1)	N(11)–Ag(1)–P	126.5(1)

1.132(8), 1.125(8) Å, C(1)–Ag(2)–C(2) 173.6(2), angles at C(1,2) 175.6(5), 178.1(6)°; about the four-co-ordinate silver(I), Ag(1)–N(1,2) are somewhat disparate and shorter than Ag(1)–N(11) (py), with an irregular geometry with the largest angle, perhaps surprisingly, N(11)(py)–Ag(1)–P (Table 5). A single unit of the polymer comprises the asymmetric unit of the structure, the polymer being generated by the 2₁ screw.

For the two polymeric structures that involve bridging NC–Ag–CN (Figs. 3 and 4) the –Ag–NC–Ag–CN– chains are non-linear, mainly because of a 'kinking' at the silver atom bearing the organic ligands. This kinking may be a consequence of the fact that the bond angles about this silver atom must be less than 180° because of its higher co-ordination number (four). Other structures (e.g. cyclic oligomers or zigzag chains) which could accommodate such a non-linear angle while maintaining all linear Ag–C–N or Ag–N–C angles are conceivable. However, the present structures, which involve kinks in an otherwise linear –Ag–NC–Ag–CN– chain (with concomitant bending of the Ag–N–C bonds involving the four-co-ordinate silver), are apparently preferred.

The 1:1 adduct of AgCN:tmpp is a pyridine hemisolvate and, like many tmpp complexes of silver(I) salts, is ionic, ligand disproportionation yielding the familiar [Ag(tmpp)₂]⁺ cation, with an [Ag(CN)₂][–] anion solvated by pyridine, [Ag(CN)₂(py)][–]: bis[tris(2,4,6-trimethoxyphenyl)phosphine]silver(I) dicyano(pyridine)argentate(I) (Fig. 5). The silver atom in the cation is located on a crystallographic 2 axis which relates the two ligands; P–Ag–P is 177.38(7)° and Ag–P 2.417(2) Å, one of the more precisely determined of such examples. The linear [NCaAgCN][–] anion, refined as C-bound but non-definitively so, lies with the silver atom close to, but not precisely coincident with, a crystallographic 2 axis, lying 0.28(2) Å from its rotation image and 1.90(2), 2.17(2) Å from the pair of associated carbon atoms, whose locations must be considered as poorly determined in the circumstances, with their large thermal envelopes, as well as those of the associated nitrogen atoms encompassing probable disorder. The angle C–Ag–C is 168.4(4)°, presumably bent from linearity in response to the approach by the solvent pyridine, which lies about the two-fold axis that passes through the nitrogen and opposite carbon. The distance Ag⋯N is long [3.16(2) Å], indicative that the interaction may simply be a consequence of a fortuitous packing, an adventitious void lying close by.

Infrared spectroscopy

Previous studies of copper(I) and silver(I) halide complexes have shown that IR spectroscopy provides a valuable tool with which to characterize them. In particular, the ν(MX) vibrational modes in the far-IR region give characteristic patterns of bands for the various types of structures that can occur for these compounds, and the wavenumbers of these modes are sensitive to the strength of the M–X bonds.^{10–16} Thus, the ν(MX) wavenumbers have been empirically correlated with the M–X bond length *r* via relationship (1) where *b* and *m* are con-

$$\nu/\text{cm}^{-1} = b(r/\text{Å})^{-m} \quad (1)$$

stants.^{12,16} Somewhat surprisingly, this relationship appears to be valid for vibrations involving both terminal and bridging

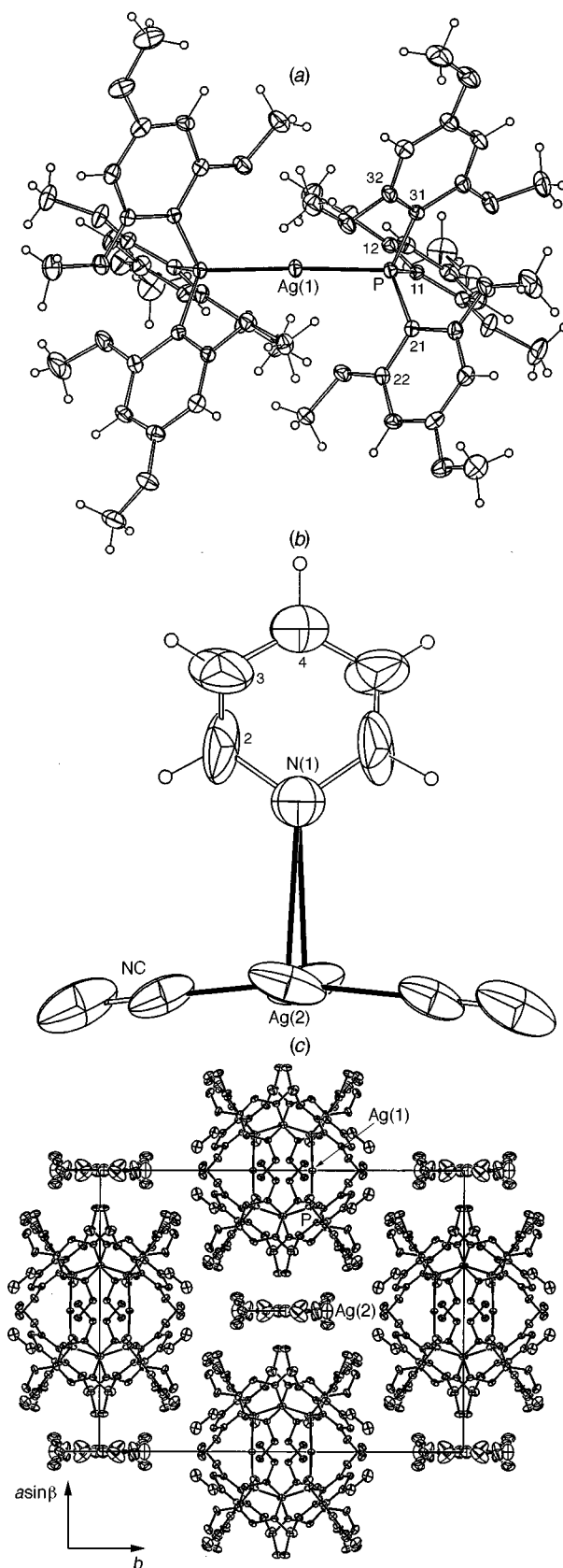


Fig. 5 (a) The [Ag(tmpp)₂]⁺ cation projected normal to its axis, (b) the associated [Ag(CN)₂(py)][–] array, projected normal to the 2 axis and (c) the unit cell contents, projected down *c*

halogen atoms X.^{13,15,16} The most likely reason for this is that the M–X–M angles in the bridged complexes are close to 90°, so that the vibrations of the two M–X bonds involved in the bridge are essentially uncoupled, and so are independent of each other.

In contrast to the situation for the halide complexes,

Table 6 The Ag–X bond distances and $\nu(\text{AgX})$, $\nu(\text{CN})$ IR band positions for some AgCN adducts containing (a) terminal and (b) bridging cyanide groups

Species	$r(\text{Ag-X})/\text{\AA}$	Ref.	$\nu(\text{AgX})/\text{cm}^{-1}$	$\nu(\text{CN})/\text{cm}^{-1}$	Ref.
(a) Terminal CN					
AgCN (monomer)	2.087	17	364	2094	17
$[\text{Ag}(\text{CN})_2]^-$	2.05	<i>a</i>	396 (IR) 360 (Raman)	2140 (IR) 2146 (Raman)	18
$[\text{Ag}\{\text{P}(\text{C}_6\text{H}_{11})_3\}_2(\text{CN})]$	2.153	14	288	2107	14 ^b
$[\text{Ag}\{\text{As}(\text{C}_6\text{H}_{11})_3\}_2(\text{CN})]$	2.14	2	311	2111	2 ^b
$[\text{Ag}\{\text{SbPh}_3\}_2(\text{CN})]$	2.090	1	310	2115	<i>b</i>
(b) Bridging CN					
$\text{AgCN}\cdot 2\text{AgNO}_3$	2.04, 2.06	19	435	2119	<i>b</i>
$[\text{Ag}(\text{SbPh}_3)_2(\text{CN})]$	2.133, 2.263	<i>b</i>	358	2133	<i>b</i>
$[\{\text{Ag}(\text{PPh}_3)_2(\text{CN})\}]^+$	2.27	<i>b,c</i>	301	2108	<i>b,c</i>
$[\{\text{Ag}(\text{AsPh}_3)_2(\text{CN})\}]^+$	2.19	<i>b,c</i>	354	2124	<i>b,c</i>

^a Average value for compounds containing this ion (see text). ^b This work. ^c For the compounds $[\{\text{Ag}(\text{EPh}_3)_2(\text{CN})\}][\text{Ag}(\text{CN})_2]\cdot 3\text{py}$ (E = P or As); the IR spectra also showed $\tilde{\nu}(\text{AgX}) = 394$ and $\tilde{\nu}(\text{CN}) = 2135, 2133 \text{ cm}^{-1}$ respectively due to the $[\text{Ag}(\text{CN})_2]^-$ ion.

relatively little is known about the M–X vibrational modes of Group 11 metal cyanides (X = CN). While the situation is expected to be similar in many respects to that of the halide complexes, the data that have been available to date have not permitted an examination of this point. Also, the cyano complexes differ from the halide complexes in the important respect that, where cyanide bridging occurs, this normally involves a linear M–CN–M arrangement, so that the vibrations of the two ‘M–X’ bonds (M–C and M–N) will be strongly coupled, in contrast to the situation for terminal M–CN bonding where the $\nu(\text{M–X})$ frequency depends only on the properties of the M–C bond. Since the present study, together with other recently published or concurrent studies, have yielded examples of AgCN complexes with a variety of structures, we have attempted to assign the $\nu(\text{M–X})$ bands in the IR spectra of a number of complexes with a view to establishing the relationship between the $\nu(\text{M–X})$ frequencies and the structures of the complexes concerned. As a starting point we summarize the results for the relatively few AgCN complexes whose vibrational spectra have been previously assigned. These data are given in Table 6.

Considering first the cases involving terminal Ag–CN bonding, the simplest example of this is the isolated triatomic Ag–CN molecule. No experimental data for this have been reported to date, but a theoretical study has yielded $\tilde{\nu}(\text{AgX}) = 364 \text{ cm}^{-1}$ for this species.¹⁷ The simplest species involving terminal Ag–CN bonding that has been well characterized experimentally is the linear $[\text{Ag}(\text{CN})_2]^-$ ion. Here the situation is complicated by the presence of coupling between the two collinear Ag–C bonds, which gives rise to two $\nu(\text{AgX})$ modes $\{396 \text{ cm}^{-1}$, IR and 360 cm^{-1} , Raman for solid $\text{K}[\text{Ag}(\text{CN})_2]\}$.¹⁸ The average $\tilde{\nu}(\text{Ag–X}) = 378 \text{ cm}^{-1}$ can be taken to be representative of this bonding situation, and it can be noted that this is quite close to the value calculated for isolated Ag–CN (Table 6). Two further species that involve well defined terminal Ag–CN bonding are $[\text{Ag}\{\text{E}(\text{C}_6\text{H}_{11})_3\}_2(\text{CN})]$ (E = P or As).^{2,14} These compounds contain monomeric units with trigonal planar E_2AgC bonding, and the IR spectra show $\tilde{\nu}(\text{Ag–X}) = 288$ and 311 cm^{-1} respectively for the Ag–C bonds. The Ag–C bond length data are available for all of the above compounds, although the value of 2.13 \AA that was originally reported for $\text{K}[\text{Ag}(\text{CN})_2]$ is considered to be rather unreliable,²⁰ and results for a range of other compounds containing $[\text{Ag}(\text{CN})_2]^-$ ions, including the ones in the present study, yield smaller values of about 2.05 \AA .²¹ This, and the other experimental data for $\text{K}[\text{Ag}(\text{CN})_2]$ and $[\text{Ag}\{\text{E}(\text{C}_6\text{H}_{11})_3\}_2(\text{CN})]$, yield a good fit using equation (1) with $b = 15\,560$, $m = 5.17$. This can be compared with the values previously determined for Ag–Cl complexes: $b = 22\,340$, $m = 5.09$.¹⁶ The best-fit curve is compared in Fig. 6 to those for the AgX (X = Cl, Br or I) complexes. The experimental data points for the AgCl com-

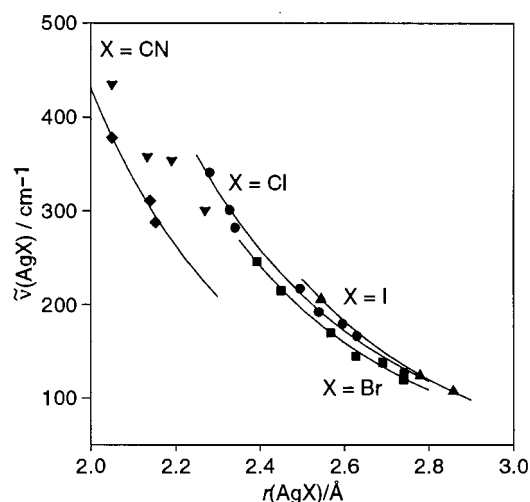


Fig. 6 Plots of the wavenumber of the $\nu(\text{AgX})$ band against Ag–X bond length. Data are for X = Cl (●), Br (■), I (▲) (from ref. 16) and for terminal (◆) and bridging (▼) CN. The curves are the best fit using equation (1) for the first four cases

plexes are the same as those reported in the previous study, with the exception that a point for $[\text{AgCl}_2]^-$ has been included. This species shows two $\nu(\text{AgCl})$ modes (333 cm^{-1} , IR and 268 cm^{-1} , Raman in tri-*n*-butyl phosphate solution).²² The average $\tilde{\nu}(\text{AgCl}) = 301 \text{ cm}^{-1}$ and the Ag–Cl bond length $2.329(2) \text{ \AA}$ ²³ yield a point that lies exactly on the curve for the other AgCl complexes (Fig. 6), and this provides some justification for the procedure that has been used to incorporate the $[\text{Ag}(\text{CN})_2]^-$ data into the correlation for the terminal Ag–CN species (see discussion above).

The simplest system that involves the linear Ag–CN–Ag bridge bonding mode is solid AgCN. This consists of infinite linear chains of Ag atoms connected by linear CN bridging groups, and a single $\nu(\text{AgX})$ mode has been assigned at 480 cm^{-1} .²⁴ The main reason for the considerable increase in frequency relative to the terminal Ag–CN case is the coupling of the Ag–C and Ag–N coordinates that occurs in the linear bridge bonding case, as discussed above. Another example of this bonding situation occurs in the compound $\text{AgCN}\cdot 2\text{AgNO}_3$.¹⁹ This contains infinite $-\text{Ag–CN–Ag–CN}-$ chains, similar to solid AgCN itself, but the chains are separated by Ag^+ and NO_3^- ions. Since no vibrational studies have been reported to date for this complex we have prepared it and recorded its far-IR spectrum (Fig. 7). The spectrum is similar to that of solid AgCN,²⁴ and by analogy with this the weak band at 435 cm^{-1} is assigned to the $\nu(\text{AgX})$ mode of the chain.

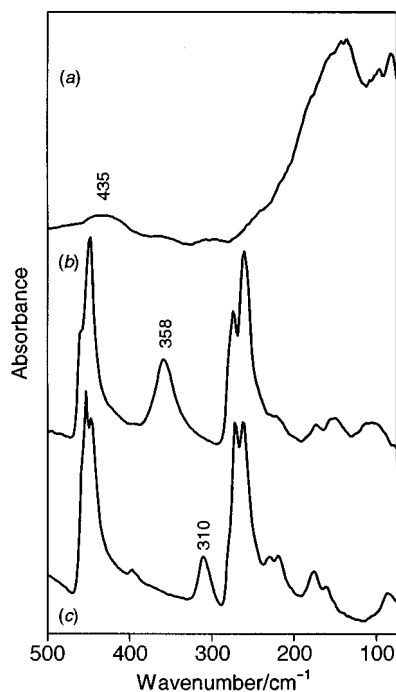


Fig. 7 Far-infrared spectra of (a) $\text{AgCN}\cdot 2\text{AgNO}_3$, (b) $[\text{Ag}(\text{SbPh}_3)_2(\text{CN})]$ and (c) $[\text{Ag}(\text{SbPh}_3)_3(\text{CN})]$. Bands assigned to the $\nu(\text{AgX})$ modes are labelled with their wavenumbers

Although the Ag–X distances for this compound are the same as those of $[\text{Ag}(\text{CN})_2]^-$, the $\nu(\text{AgX})$ frequency is considerably higher (Table 6, Fig. 6). This is due to the fact that this frequency depends on the sum of the Ag–C and Ag–N force constants in the Ag–CN–Ag bridge, due to coupling of these coordinates as discussed above. Thus, it is not possible to represent the frequencies of the bridging $\nu(\text{AgX})$ modes by an equation of the type (1), since these frequencies depend on the strengths of the two bonds involved in the bridge. Nevertheless, the above result suggests that the frequencies of bridging CN groups will be greater than those of terminal CN groups for similar Ag–C bond lengths.

This latter point is well illustrated by the results for $[\text{Ag}\{\text{Sb}(\text{PPh}_3)_3\}_n(\text{CN})]$ ($n = 2$ or 3). The far-IR spectra of these compounds are shown in Fig. 7. These show strong bands at about 450 and 270 cm^{-1} due to the co-ordinated Ph_3Sb .^{25,26} The bands at 358 and 310 cm^{-1} for the $n = 2$ and 3 compounds respectively are assigned as the $\nu(\text{AgX})$ modes of the CN groups. Initially it was rather surprising to find that the wavenumber for the $n = 2$ compound is greater than that for $n = 3$, as the Ag–C bond length in the latter compound is shorter than that in the former (Table 6), thus indicating a weaker bond. This apparent anomaly is attributed to the effects of linear bridging, as discussed above. The $n = 2$ complex has an infinite chain structure with bridging CN groups, whereas the $n = 3$ complex contains terminally bound CN. While the data for the $n = 3$ complex lie close to the best fit line for terminally bound CN [the wavenumber predicted from equation (1) is 344 cm^{-1}], those for the $n = 2$ complex lie considerably above this line [the wavenumber predicted from equation (1) using $r(\text{AgC}) = 2.133 \text{ \AA}$ is only 310 cm^{-1}]. Fig. 6 shows that the frequencies for both of the infinite chain compounds that contain bridging CN groups are about 50 cm^{-1} higher than those for analogous compounds that involve terminal CN bonding. This provides a clear contrast to the situation for the $\nu(\text{AgX})$ modes of halide complexes, where angular rather than linear bridging occurs, and the data for both types of complex lie on the same curve, as shown in Fig. 6.

The far-IR spectra of the ionic 1:2 adducts $[\{\text{Ag}(\text{EPh}_3)_3\}_2\text{CN}]^+[\text{Ag}(\text{CN})_2]^- \cdot 3\text{py}$ ($\text{E} = \text{P}$ or As) are shown in Fig. 8. These spectra show bands due to co-ordinated EPh_3 , which can be assigned with reference to the spectra of uncomplexed EPh_3 .^{25,26}

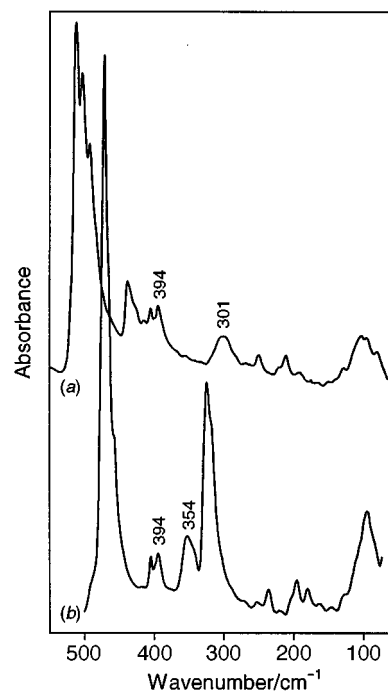


Fig. 8 Far-infrared spectra of $[\{\text{Ag}(\text{EPh}_3)_3\}_2\text{CN}]^+[\text{Ag}(\text{CN})_2]^- \cdot 3\text{py}$: (a) $\text{E} = \text{P}$, (b) $\text{E} = \text{As}$. Bands assigned to the $\nu(\text{AgX})$ modes are labelled with their wavenumbers

They also show a band at 394 cm^{-1} that can be assigned to the antisymmetric $\nu(\text{AgC})$ mode of $[\text{Ag}(\text{CN})_2]^-$ {cf. 396 cm^{-1} for $\text{K}[\text{Ag}(\text{CN})_2]$.¹⁸ We have assigned the bands at 301 and 354 cm^{-1} in the $\text{E} = \text{P}$ and As compounds respectively to the $\nu(\text{AgX})$ modes of the linear bridging CN groups in the cations. The increase in wavenumber from $\text{E} = \text{P}$ to As is in agreement with the trend in Ag–CN bond lengths, Table 6. These data are included in the plot of $\nu(\text{AgX})$ vs. $r(\text{AgX})$ in Fig. 6. This shows that, as in the case of the compounds with infinite chain structures, the frequencies for these compounds are significantly higher (in this case by about 80 cm^{-1}) than those for analogous compounds that involve terminal CN bonding. Again, this can be attributed to the effects of linear bridging, as discussed above. Thus, while the behaviour of the $\nu(\text{AgX})$ modes in cyano-complexes ($\text{X} = \text{CN}$) is clearly more complicated than that of halogeno complexes ($\text{X} = \text{Cl}, \text{Br}$ or I), the data obtained for the present series of complexes provide a good basis for understanding this unusual behaviour.

The $\nu(\text{CN})$ wavenumbers for several of the compounds prepared in this study were measured from their IR spectra, and the values are compared with those of some related compounds in Table 6. The relationship between $\nu(\text{CN})$ and $r(\text{AgX})$ for the AgCN/ER_3 complexes is shown in Fig. 9. From this it is clear that there is some overlap between the range of $\nu(\text{CN})$ values for the terminal and bridging bonding modes of the CN group, although the values for the bridging groups tend to be higher. There is a clear trend of increasing $\nu(\text{CN})$ with decreasing $r(\text{AgX})$, and the rate of this increase is greater for the bridging than for the terminal bonding mode. These results can readily be explained in terms of the Ag/CN bonding interactions; co-ordination of the CN group by σ donation to a silver atom results in an increase in $\nu(\text{CN})$. For a given Ag–X bond length the effect on $\nu(\text{CN})$ is greater in the bridging mode, since two silver atoms are acting as electron acceptors. Hence the correlation line for bridging should lie above that for terminal bonding, and the rate of increase should be greater for the bridging case, as observed. One as yet unexplained anomaly concerning the results in Table 6 is the relatively low $\nu(\text{CN})$ for $\text{AgCN}\cdot 2\text{AgNO}_3$. In this compound AgCN forms linear chains with bridging CN groups, as has also been proposed for solid

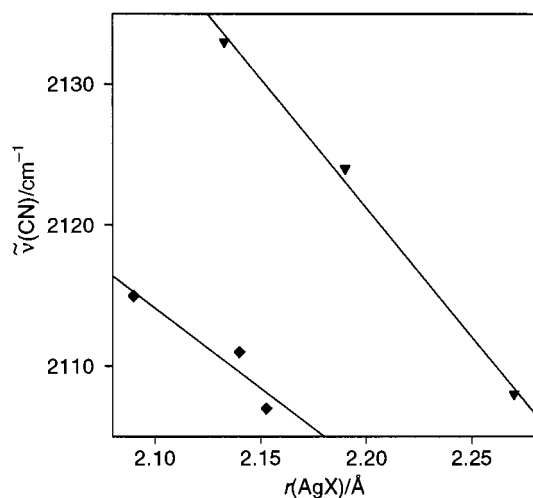


Fig. 9 Plots of the wavenumber of the $\nu(\text{CN})$ band against Ag-X bond length for AgCN/ER_3 complexes containing terminal (\blacklozenge) and bridging (\blacktriangledown) CN groups

AgCN itself.^{19,24} Extrapolation of the correlation line for bridging bonding (Fig. 9) to the $r(\text{AgX})$ value reported for $\text{AgCN}\cdot 2\text{AgNO}_3$ yields a $\nu(\text{CN})$ value that is considerably higher than the observed value of 2119 cm^{-1} (Table 6). However, a similar extrapolation for solid AgCN itself yields a value close to the observed $\tilde{\nu}(\text{CN}) = 2168\text{ cm}^{-1}$ for this compound,²⁴ suggesting that the anomaly in the $\text{AgCN}\cdot 2\text{AgNO}_3$ adduct is peculiar to this compound.

Acknowledgements

We acknowledge support of this work by grants from the Australian Research Grants Scheme and the University of Auckland Research Committee. We thank Ms. Catherine Hobbs for recording some of the far-IR spectra, and Dr. L.-J. Baker for assistance with the X-ray crystallography.

References

- 1 Effendy, J. D. Kildea and A. H. White, *Aust. J. Chem.*, 1997, **50**, 587.
- 2 G. A. Bowmaker, Effendy, B. W. Skelton and A. H. White, *J. Chem. Soc., Dalton Trans.*, 1998, 2123.

- 3 G. A. Bowmaker, Effendy, P. C. Junk and A. H. White, *J. Chem. Soc., Dalton Trans.*, preceding paper.
- 4 D. E. Hibbs, M. B. Hursthouse, K. M. Malik, M. A. Beckett and P. W. Jones, *Acta Crystallogr., Sect. C*, 1996, **52**, 884.
- 5 L. M. Engelhardt, P. C. Healy, V. A. Patrick and A. H. White, *Aust. J. Chem.*, 1987, **40**, 1873.
- 6 G. A. Bowmaker, Effendy, J. V. Hanna, P. C. Healy, B. W. Skelton and A. H. White, *J. Chem. Soc., Dalton Trans.*, 1993, 1387.
- 7 G. A. Bowmaker, Effendy, E. N. de Silva and A. H. White, *Aust. J. Chem.*, 1997, **50**, 627, 641.
- 8 M. M. Olmstead, G. Speier and L. Szabó, *J. Chem. Soc., Chem. Commun.*, 1994, 541.
- 9 S. Gotsis, L. M. Engelhardt, P. C. Healy, J. D. Kildea and A. H. White, *Aust. J. Chem.*, 1989, **42**, 923; corrigendum, Effendy, L. M. Engelhardt, P. C. Healy, B. W. Skelton and A. H. White, *Aust. J. Chem.*, 1991, **44**, 1585.
- 10 B. K. Teo and D. M. Barnes, *Inorg. Nucl. Chem. Lett.*, 1976, **12**, 681.
- 11 G. A. Bowmaker and P. C. Healy, *Spectrochim. Acta, Part A*, 1988, **44**, 115.
- 12 G. A. Bowmaker, P. C. Healy, J. D. Kildea and A. H. White, *Spectrochim. Acta, Part A*, 1988, **44**, 1219.
- 13 G. A. Bowmaker, R. D. Hart, B. E. Jones, B. W. Skelton and A. H. White, *J. Chem. Soc., Dalton Trans.*, 1995, 3063.
- 14 G. A. Bowmaker, Effendy, P. J. Harvey, P. C. Healy, B. W. Skelton and A. H. White, *J. Chem. Soc., Dalton Trans.*, 1996, 2449.
- 15 G. A. Bowmaker, Effendy, P. J. Harvey, P. C. Healy, B. W. Skelton and A. H. White, *J. Chem. Soc., Dalton Trans.*, 1996, 2459.
- 16 G. A. Bowmaker, Effendy, J. D. Kildea and A. H. White, *Aust. J. Chem.*, 1997, **50**, 577.
- 17 F. C. Veldkamp and G. Frenking, *Organometallics*, 1993, **12**, 4613.
- 18 T. M. Loehr and T. V. Long, *J. Chem. Phys.*, 1970, **53**, 4182.
- 19 D. Britton and J. D. Dunitz, *Acta Crystallogr.*, 1965, **19**, 815.
- 20 A. G. Sharpe, *The Chemistry of Cyano Complexes of the Transition Metals*, Academic Press, London, 1976, p. 274.
- 21 C. Kappenstein, A. Quali, M. Guerin, J. Cernak and J. Chomic, *Inorg. Chim. Acta*, 1988, **147**, 189; M. Carcelli, C. Ferrari, C. Pelizzi, G. Pelizzi, G. Predieri and C. Sollinas, *J. Chem. Soc., Dalton Trans.*, 1992, 2127; J. Cernak, M. Kanuchova, J. Chomic, I. Potocnak, J. Kamenicek and Z. Zak, *Acta Crystallogr., Sect. C*, 1994, **50**, 1563.
- 22 D. N. Waters and B. Basak, *J. Chem. Soc. A*, 1971, 2733.
- 23 G. Helgesson and S. Jagner, *Inorg. Chem.*, 1991, **30**, 2574.
- 24 G. A. Bowmaker, B. J. Kennedy and J. C. Reid, *Inorg. Chem.*, 1998, submitted.
- 25 K. Shobatake, C. Postmus, J. R. Ferraro and K. Nakamoto, *Appl. Spectrosc.*, 1969, **23**, 12.
- 26 F. W. Parrett, *Spectrochim. Acta, Part A*, 1970, **26**, 1271.

Received 6th February 1998; Paper 8/01085D